Journal Name

Catalysis Science & Technology

ARTICLE TYPE

Cu²⁺-doped zeolitic imidazolate frameworks (ZIF-8): Efficient and stable catalysts for cycloadditions and condensation reactions

Aleksandra Schejn,[a] Abdelhay Aboulaich,[b] Lavinia Balan,[c] Véronique Falk,[a] Jacques Lalevée,[c] Ghouti Medjahdi,[d] Lionel Aranda,[d] Kevin Mozet,[a] Raphaël Schneider[*a]

5

Cu²⁺-doped zeolitic imidazolate frameworks (ZIFs) crystals were efficiently prepared by reaction of Cu(NO₃)₂, Zn(NO₃)₂, and 2-methylimidazole in methanol at room temperature. Scanning electron
10 microscopy, transmission electron microscopy and X-ray diffraction showed that the Cu/ZIF-8 particles were nanosized (between ca. 120 and 170 nm) and that the body-centered cubic crystal lattice of the parent ZIF-8 framework is continuously maintained, regardless of the doping percentage. Moreover, thermogravimetric analyses and specific BET surface area measurements demonstrated that the doping doesn't alter the high stability of ZIF-8 crystals and that the porosity only decreases at a high doping
15 percentage (25% in Cu²⁺). The Cu/ZIF-8 material showed excellent catalytic activity in the [3+2] cycloaddition of organic azides with alkynes and in Friedländer and Combes condensations due to the high catalyst surface area and the high dispersion of Cu/ZIF-8 particles. Notably, the Cu/ZIF-8 particles not only exhibit excellent performances but also had a great stability in the reaction, allowing their reuse up to ten times in condensation reactions. Our findings explored a simple and powerful way to
20 incorporate metal ions into the backbones of open framework materials without losing their properties.

Introduction

Metal-organic frameworks (MOFs), which are porous crystalline materials consisting of metal ions or metal containing clusters coordinated to rigid organic molecules to form one-, two-, or 25 three-dimensional networks, have attracted great attention due to their exceptional high surface area, high porosity, low density, and chemically tunable structures.[1-8] Among MOFs, the so-called zeolitic imidazolate frameworks (ZIFs) are extremely promising materials because they combine the pore size tunability of MOFs 30 and the thermal stability of zeolites making them ideal candidates for applications such as gas storage,[9,10] gas separation,[6,11] catalysis[12] or drug delivery.[13] ZIFs are constructed from tetrahedral units, in which each metal atom such as Zn^{2+} or Co^{2+} connects four imidazolate (im⁻) ligands to form neutral 35 frameworks.[14-20] ZIF-8 ($Zn(mim)_2$, mim⁻ = 2-methylimidazolate), with the sodalite (SOD) topology, crystallizes in the cubic space group $I\overline{4}3m$ with a lattice constant of 16.992 Å and contains 276 atoms in the unit cell ($Zn_{12}N_{48}C_{96}H_{120}$). The sodalite cages possess a pore diameter of 11.6 Å and the aperture between two 40 cages is 3.4 Å. ZIF-8 crystals are typical porous MOFs with unusual high thermal and chemical stability, as well as tunable zeotype topologies.[2,14-19]

While the incorporation of metal or semiconductor nanoparticles into the ZIF framework is now well-documented,[20-25] 45 substitutional introduction of metal cations in the crystalline lattice has far less been studied. In the course of our studies related to the construction of ZIF-8 derived hybrid materials

displaying sorptive, magnetic and/or catalytic properties, we sought to investigate the consequences of Cu²⁺ doping on the 50 ZIF-8 framework. ZIF-8 is a wide bandgap material (bandgap energy Eg = 4.9 eV) and adsorbs only in the UV region.[26] Doping copper into ZIF-8 should not only allow to engineer its bandgap and displace its absorption into the visible-light area, but also to develop new nanomaterials combining both the catalytic and 55 magnetic properties of Cu²⁺ and the high thermal and chemical stability of ZIF-8 crystals. For example, the presence of Cu²⁺ ions in the ZIF-8 structure should enable their use as reusable catalysts for coupling reactions and oxidation-reduction reactions, as recently described for Cu(im)₂,[27,28] CuBTC[29] (Basolite[TM] C300, 60 BTC = 1,3,5-benzene tricarboxylate) and Fe(BTC).[30] The association of Cu²⁺ ions with imidazole or its derivatives as ligands/linkers to construct MOFs[27,28,31-46] or coordination polymers[47,48] is well-established. The doping in copper of ZIF-67 (Co(im)₂) and the photocatalytic properties of the Cu/ZIF-67 65 crystals under visible light irradiation have recently been reported.[49] Very recently, Li *et al.* reported also the successful incorporation of six-coordinated nickel(+2) clusters into ZIF-8 crystals cavities.[50,51] The materials prepared found applications in alcohol sensing or carbon dioxide capture and separation after 70 pyrolysis. So far, Cu²⁺-doping into $Zn(im_2)_2$ (ZIF-1) has only been described one time,[52] and Cu²⁺-doping into ZIF-8 has never been explored.

In this work, we report the successful preparation of Cu-doped ZIF-8 crystals and the application of these substitutionally doped 75 particles as efficient heterogeneous catalysts for copper-catalyzed Huisgen 1,3-dipolar cycloadditions and for Friedländer and Combes condensations. These catalytic activities were gained

without alteration of the stability of ZIF-8 crystals and with only a slight decrease of the specific area and pore size at high dopant percentage (25% Cu relative to Zn). The Cu/ZIF-8 crystals could be separated from the reaction mixture by simple centrifugation and could be reused up to ten times without a significant alteration in catalytic activity.

Experimental

Materials

Zinc nitrate hexahydrate (98%, Aldrich), copper nitrate trihydrate (99.5%, Merck), 2-methylimidazole Hmim (99%, Aldrich), acetylacetone (99%, Aldrich), 2-aminobenzophenone (98%, Aldrich), aniline (99.5%, Aldrich), benzyl bromide (≥ 98%, Fluka), sodium azide (≥ 99.5%, Aldrich), phenyl acetylene (> 98%, Alfa Aesar), ethynyltrimethylsilane (98%, Aldrich), 1-octyl bromide (99%, Aldrich), methyl 5-bromovalerate (97%, Aldrich), sodium chloride (99-100.5%, Carlo Erba), sodium sulphate (≥ 99%, Carlo Erba), DMSO (≥ 99.7%, Fisher), ethanol (≥ 99.8%, Aldrich), methanol (≥ 99,9%, Aldrich), toluene (≥ 99%, Prolabo), diethyl ether (≥ 99.5%, Aldrich) were used as received without any further purification. DI water (18.2 MΩ·cm) was used in all experiments. Benzyl azide, 1-octyl azide and methyl 5-azidovalerate were prepared according to the synthetic protocol described in reference 53.

Synthesis of Cu-doped ZIF-8

A solution of the $Zn(NO_3)_2$ and $Cu(NO_3)_2$ (total 1 mmol) in 11.3 mL methanol and Hmim (660 mg, 8 mmol) in the same volume of methanol were prepared separately. Then, in a three-neck-flask, the two solutions were mixed by dropwise addition of the Hmim solution to the Zn^{2+} and Cu^{2+} solution. The synthesis was conducted under nitrogen flow at room temperature with stirring for 1 h. The Cu-doped ZIF-8 crystals were separated by centrifugation (4000 rpm, 15 min) and washed with methanol (3 × 30 mL). The material was dried at room conditions overnight before analysis. To use the material in catalytic reactions, the Cu/ZIF-8 samples were activated by treatment of the powders at 200°C in a programmable oven for 6 h, and then cooled to room temperature naturally. The vials containing the Cu/ZIF-8 powders were tightly capped and stored at room temperature before use.

Friedländer reaction

2-Aminobenzophenone (82.1 mg, 0.42 mmol) and ethyl acetoacetate (81.3 mg, 0.62 mmol, 1.48 equiv.) were added to Cu/ZIF-8 crystals (8 mol% of catalyst) dispersed in 2 mL of toluene. The mixture was stirred at 90°C and the progress of the reaction was monitored by TLC. After cooling, the reaction mixture was centrifuged and the toluene phase concentrated. The product was purified by flash chromatography and analyzed with ^{1}H and ^{13}C NMR.

Combes reaction

The catalysis was conducted in a solvent-free environment. Briefly, aniline (1 mmol) and acetylacetone (5 mmol) were mixed

with 8 mol% of the Cu/ZIF-8 catalyst at 100°C for 3 h. Then, the catalyst was separated by centrifugation (4000 rpm, 15 min), washed three times with toluene and dried. The reaction mixture was centrifuged and the toluene phase concentrated. The product was purified by flash chromatography and analyzed with ^{1}H and ^{13}C NMR.

### Huisgen's dipolar cycloaddition

Click reactions were conducted according to a slightly modified literature procedure.[27] The general protocol for 1,3-dipolar cycloaddition of the azides to the alkynes was as follows. The Cu/ZIF-8 catalyst (5 mol% of catalyst) in ethanol (6 ml) was placed inside a round bottom flask connected to a reflux condenser and the temperature was set to 70 °C under argon. Azide (1 mmol) and alkyne (1.2 mmol) were then added and the mixture was stirred during 3 h. Then the catalyst was isolated by centrifugation, washed with ethanol and dried. The product was purified by flash chromatography and analyzed with ^{1}H and ^{13}C NMR.

Characterization

Transmission electron microscopy (TEM) images were taken by placing a drop of the ZIF-8 particles in methanol onto a carbon film-supported copper grid. Samples were studied using a Philips CM20 instrument operating at 200 kV. Scanning electron microscopy (SEM) pictures were prepared using JEOL Scanning Electron Microscope JSM-6490 LV. The X-ray powder diffraction data were collected from an X'Pert MPD diffractometer (Panalytical AXS) with a goniometer radius 240 mm, fixed divergence slit module (1/2° divergence slit, 0.04 rd Sollers slits) and an X'Celerator as a detector. The powder samples were placed on a silicon zero-background sample holder and the XRD patterns were recorded at room temperature using Cu K_α radiation (λ = 0.15418 nm). The textural properties of the materials were investigated with a Micromeritics ASAP 2420 instrument using liquid nitrogen (-196 °C). Prior to the analyses, the samples were out-gassed overnight in vacuum at 40°C on the degassing port followed by 4 h out-gassing on the analyse port. The resulting isotherms were analysed using the BET (Brunauer-Emmett-Teller) method while the micropore volume (V_{micro}) was determined using the Horvath-Kawazoe (HK) equation. The surface areas, pore volumes and pore sizes determined (see Table 1) are the average of two independent measurements. Thermogravimetric measurements were performed on a SETARAM Setsys Evolution thermoanalyzer coupled with an Omnistar GSD301C-Pfeiffer Vacuum mass spectrometer. Samples were filled into platinum crucibles and heated in a flow air with a ramp of 5°C.min^{-1} from room temperature up to 800°C. ^{1}H NMR spectra were recorded in $CDCl_3$ using a 300 MHz spectrometer (Avance 300, Bruker, Bremen, Germany). Diffuse reflectance UV-vis spectra of the samples were measured using a Shimadzu UV-2101 PC spectrophotometer. $BaSO_4$ is used as a standard for baseline measurements and spectra are recorded in a range of 200-1400 nm. A VARIAN 720-ES Inductively Coupled Plasma-Optical Emission Spectrometer (ICP-OES) was used for multi-elemental analyses. ESR experiments were carried out using a X-Band EMX-plus spectrometer (Bruker Biospin). The

samples were investigated at room temperature. The double integration of the ESR spectrum is proportional to the

concentration in paramagnetic centers.[54] A calibration was first done using 2,2,6,6-
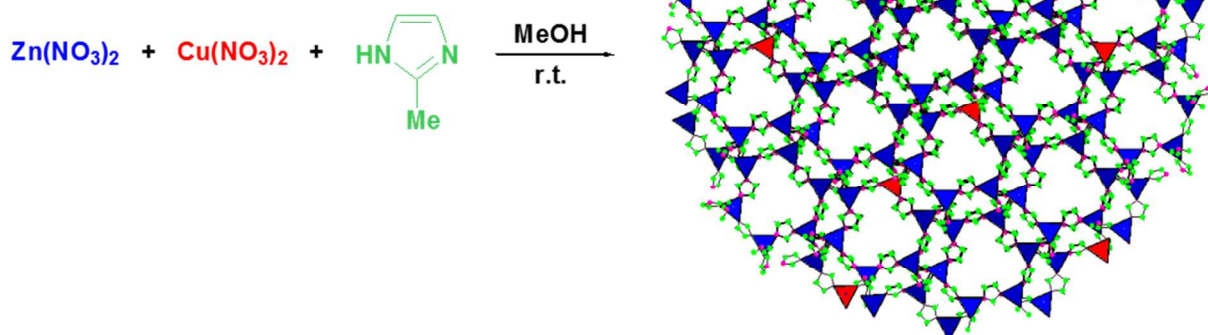
Scheme 1 Schematic representation of the synthesis of Cu-doped ZIF-8 crystals.

Fig. 1 Photographs showing the color change of Cu/ZIF-8 crystals upon increasing the doping percentage in copper. (a) ZIF-8 as reference, (b), (c), (d) and (e) are ZIF-8 crystals doped with 1, 5, 10 and 25% Cu, respectively.

tetramethylpiperidine-1-oxyl (TEMPO) to ensure that this procedure was usable in solid state. TEMPO was also used as standard for calibration (g = 2.0061).

Results and discussion

Cu-doped ZIF-8 crystals synthesis

The synthesis of Cu/ZIF-8 crystals was performed under solvothermal conditions by mixing $Zn(NO_3)_2$, $Cu(NO_3)_2$ and Hmim in ethanol at room temperature for 1 h (Scheme 1).[19,55] Molar percentages of 1, 5, 10 and 25% of $Cu(NO_3)_2$ to $Zn(NO_3)_2$ were used in these experiments. The crystals prepared will be noted $Cu_{1\%}$/ZIF-8, $Cu_{5\%}$/ZIF-8, $Cu_{10\%}$/ZIF-8, and $Cu_{25\%}$/ZIF-8 thereafter. The incorporation of Cu^{2+} ions in the crystal lattice weakly slows down the kinetics of ZIF-8 particles precipitation (*vide infra*). It is also worth to mention that a complete collapse of ZIF-8 structure was observed at higher doping percentage (50%). The crystals obtained after reaction were recovered by centrifugation, washed and dried before characterization. A significant observation is that the color intensity of the samples and the strength of their main absorption bands (*vide infra*) correlate qualitatively with their Cu^{2+} content. As shown in Fig. 1, upon increasing the doping percentage in Cu^{2+} from 1 to 25%,

the color changed from white to brown beige.

Cu-doped ZIF-8 nanocrystals characterization

When preparing pure ZIF-8 crystals from $Zn(NO_3)_2$, the solution became cloudy within 2 min after the addition of Hmim and a dense precipitate was obtained after 1 h of reaction. With the increase of the copper content in the reaction medium, the precipitate became less dense, thus indicating that the number of nuclei generated by the complex formation decreased. This was confirmed by TEM and SEM experiments (Fig. 2 and 3 and Fig. S1 for size distributions). With increasing the Cu^{2+} doping percentage in the nanocrystals, the average diameters were found to increase from ca. 120 to 170 nm. This confirms that less nuclei were formed upon addition of Hmim and that Cu-doped ZIF-8 crystals initially formed grow through further addition of single
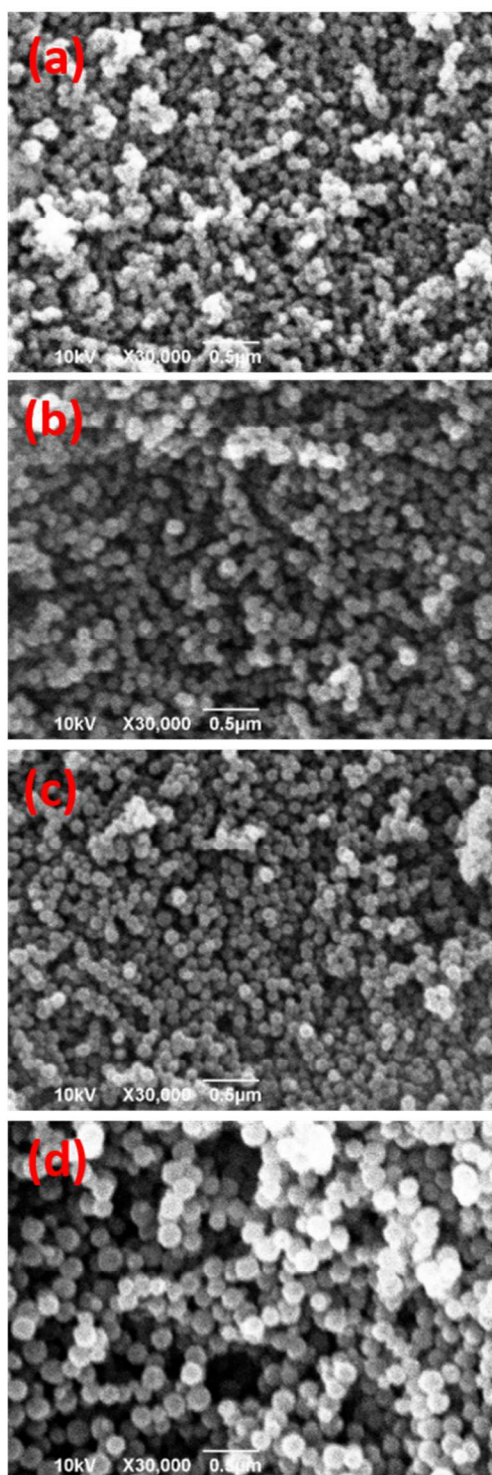
Fig. 2 SEM images of ZIF-8 crystals doped with (a) 1, (b) 5, (c) 10 and (d) 25% Cu^{2+}, respectively.

ICP-OES

Fig. 3 TEM images of ZIF-8 crystals doped with (a) 1, (b) 5, (c) 10 and (d) 25% Cu^{2+}, respectively.

monomeric mim$^-$ and solvated Zn^{2+} and Cu^{2+} species until the framework is formed. Regardless of the doping percentage, TEM and SEM images showed rather small and monodispersed nanoparticles with a well-defined truncated rhombic dodecahedron structure, which is the typical ZIF-8 morphology. Inductively coupled plasma-optical emission spectrometry (ICP-OES) was used to determine the final copper content of Cu/ZIF-8 crystals for further characterization and catalytic experiments.
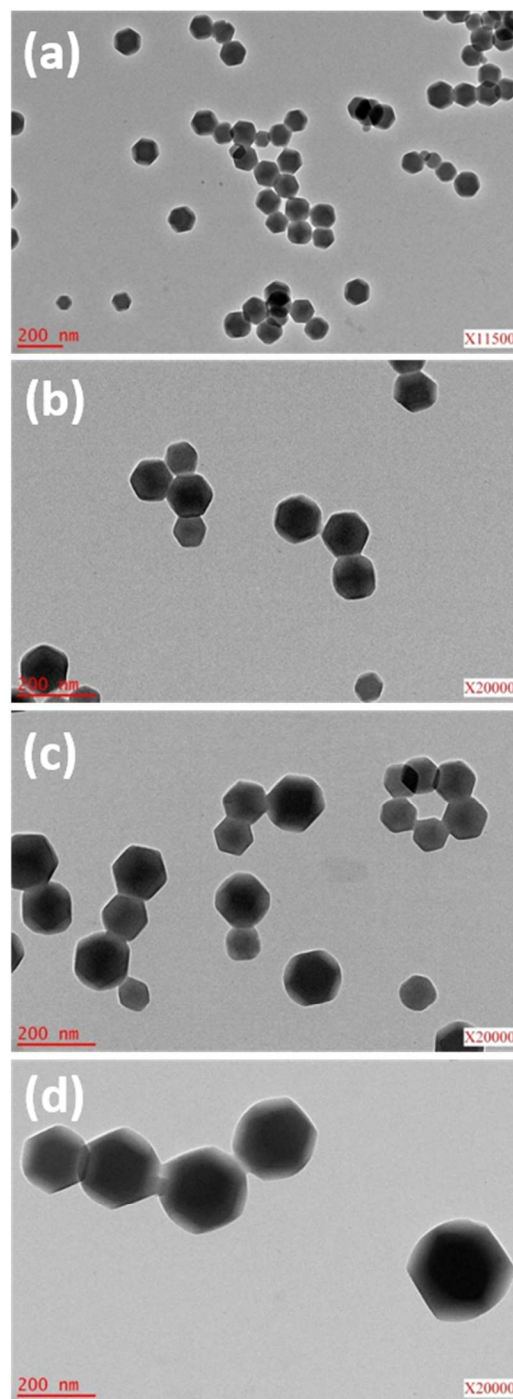
reveals that the Cu/Zn ratios for all samples are lower than Cu/Zn ratios used for the synthesis, irrespective for the dopant percentage (the Cu^{2+} doping percentage in the crystals are 0.6, 2.1, 3.9, to 8.7% for reactions conducted with 1, 5, 10, and 25% Cu^{2+}, respectively).

Powder X-ray diffraction (XRD) patterns of ZIF-8 and Cu/ZIF-8 crystals are shown in Fig. 4. For all the samples, the Cu/ZIF-8 crystals show a body-centered cubic crystal lattice group $I\bar{4}3m$ with a cell parameter a varying between 17.015 et 17.025 Å,

which is in good accordance with the results reported for ZIF-8 in the literature.[14,56] A slight decrease of the full-width at half-maximum
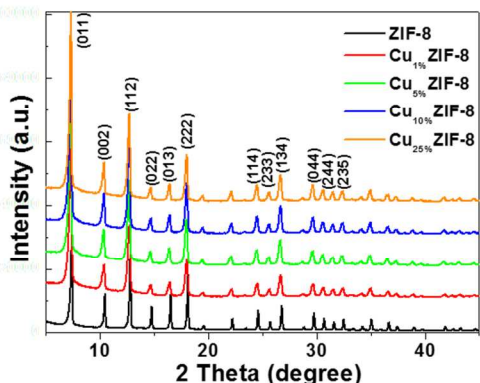

Fig. 4 XRD patterns of Cu/ZIF-8 crystals prepared with different doping percentages in Cu^{2+}.

of the (011) peak intensity was also observed when increasing the Cu doping percentage, which is consistent with the crystals size increase observed by TEM and SEM. Ni-substituted ZIF-8 crystals prepared via mechanochemical synthesis exhibited extra peaks in XRD patterns that were assigned to the clusters formed between Ni(+2) ions and Hmim that are trapped in ZIF-8 cavities.[50,51] These extra peaks were not observed in our solution phase synthesis, thus indicating that Cu^{2+} ions are probably substitutionally doped in ZIF-8 crystals.

Results depicted in Fig. 4 demonstrate that the presence of Cu^{2+} in the reaction medium during the growth of ZIF-8 crystals did not cause any structure alteration and that ZIF-8 materials still retained crystalline integrity after being doped with Cu^{2+}. It is likely that the doping with Cu^{2+} does not distort the lattice structure of ZIF-8 crystals since the ionic size of Cu^{2+} (0.71 Å) is only slightly smaller than that of Zn^{2+} (0.74 Å) in tetrahedral coordination. Finally, it is worth to mention that Cu^{2+} ions have been demonstrated to damage the crystallinity of ZIF-8 once added to these nanocrystals in aqueous solution due to interactions between Cu^{2+} ions and the mim⁻ linkers.[57] Such alterations were not observed under our experimental conditions. The presence of Cu^{2+} in the samples was further confirmed by UV-visible spectroscopy (Fig. 5). From the diffuse reflectance spectra and the corresponding absorption spectra of pure ZIF-8 and Cu-doped ZIF-8 crystals (Fig. 5a and 5b), it can be seen that doping shifts the adsorption edge of ZIF-8 crystals from the UV to the visible region. The absorption spectra of Cu-doped ZIF-8 crystals exhibit a first well-defined band located at ca. 490 nm and a second broad one starting at 600 nm and going to the infrared with a shoulder at ca. 850 nm. These bands can both be attributed to d-d transitions of Cu(+2) ions and confirm the heterobimetallic nature of the ZIF materials produced. The slight differences observed in the absorption spectra compared to Cu(+2)/imidazolate complexes described in the literature may originate from different coordination geometries around Cu(+2) ions.[58,59] Additionally, reflectance and absorption spectra of all Cu/ZIF-8 crystals exhibit the same bands, demonstrating that the structures of these materials are the same regardless of the doping

percentage. ZIF-8 is a wide band gap material with a band gap energy equal to 4.9 eV.[26] The band gap energies of the Cu/ZIF-8 samples have been determined from the absorbance [F(R)] spectra using the Kubelka-Munk formalism and Tauc plot. For indirect
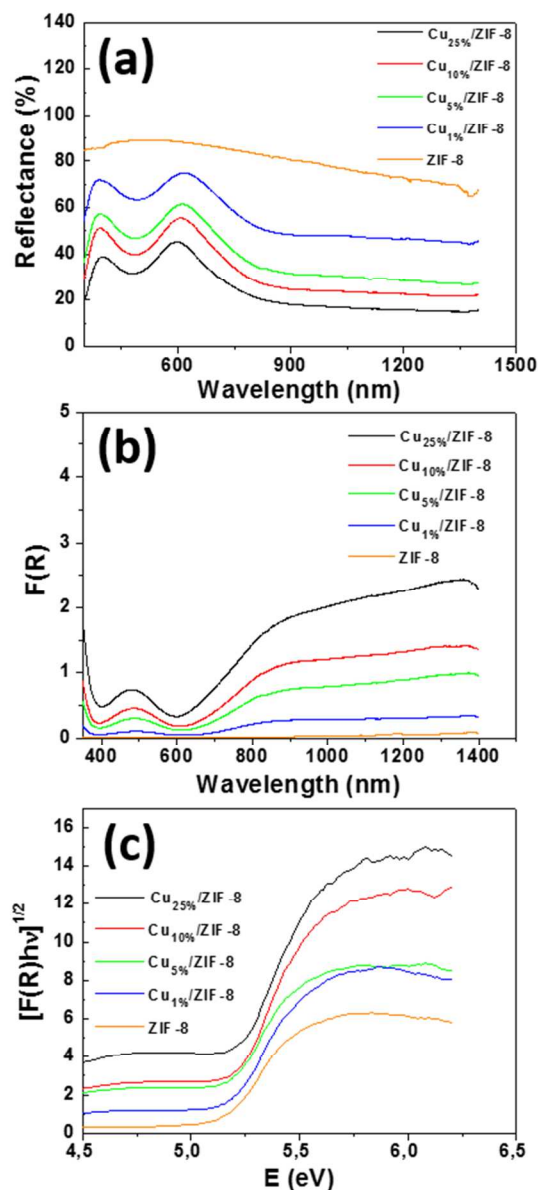

Fig. 5 (a) Diffuse reflectance and (b) absorption spectra of ZIF-8 and Cu-doped ZIF-8 crystals, and (c) $[F(R)h\nu]^{1/2}$ vs hv curves for ZIF-8 and Cu/ZIF-8 crystals.

band gap semiconductors, the energy band gap can be estimated from the tangent line in the plot of the square root of Kubelka-Munk functions F(R) against photon energy, as shown in Fig. 5c. The tangent lines, which are extrapolated to $(F(R))^{1/2} = 0$, indicate that the band gaps of $Cu_{1\%}$/ZIF-8, $Cu_{5\%}$/ZIF-8, $Cu_{10\%}$/ZIF-8, and $Cu_{25\%}$/ZIF-8 are 5.09, 5.07, 5.04, and 4.92 eV, respectively, while the band gap of undoped ZIF-8 is equal to 5.10 eV. These results are in agreement with the emergence of strong absorption bands within ZIF-8 after Cu^{2+} doping. The results are also in line with

the stronger absorption intensity observed with increasing Cu^{2+} doping as shown in Fig. 5b.

The ESR spectra of the Cu/ZIF-8 crystals are shown in Fig. 6a. The spectra exhibit one intense signal in the high field and four well-resolved peaks in the low field region, which corroborate the presence of Cu(+2) in the materials. Interestingly, the double
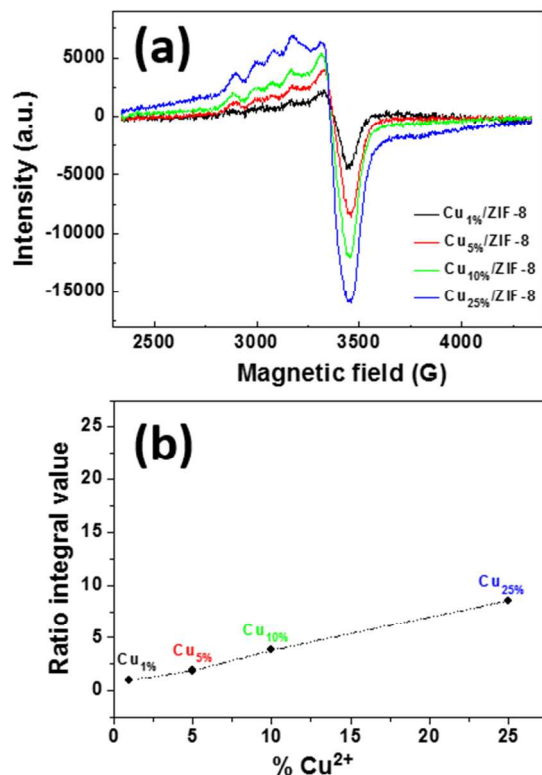

Fig. 6 (a) ESR spectra for the different Cu/ZIF-8 samples and (b) double integration of the ESR spectrum vs. Cu doping.

integration of the ESR spectra increases linearly with the Cu doping (Fig. 6b). The Cu/Zn ratios estimated by ESR (1.0, 1.87, 3.81 and 8.54% Cu^{2+} for $Cu_{1\%}$/ZIF-8, $Cu_{5\%}$/ZIF-8, $Cu_{10\%}$/ZIF-8, and $Cu_{25\%}$/ZIF-8 crystals, respectively) are in good agreement with values determined by ICP-OES (*vide supra*).

Porosity and stability of Cu/ZIF-8 crystals

After out-gassing the samples overnight in vacuum at 40°C, permanent porosities of Cu/ZIF-8 materials were demonstrated by N_2 adsorption at 77K (Fig. 7). Type I isotherms were obtained for the four Cu/ZIF crystals with BET surface areas of 1541, 1736, 1639, and 1205 $m^2.g^{-1}$ for 1, 5, 10 and 25% Cu doping, respectively, indicating microporous structure (Table 1). This structure was further confirmed by the increase in the volume adsorbed at low relative pressures ($P/P_0 < 0.08$). The adsorption-desorption hysteresis loop of N_2 near $P/P_0 = 1$, which originates from interparticle mesopores, is consistent with the interparticle voids and further confirms the dual micro- and mesoporosity of Cu/ZIF crystals.[60] Until 10% of doping in Cu^{2+}, the crystals properties were only slightly affected by the Cu^{2+} substitution. Surface areas and micropore volumes correspond well with those of pure ZIF-8 (S_{BET} = 1700 m^2g^{-1} and V_{micro} = 0.63 cm^3g^{-1}) (Table

1).[14,19] The BET surface areas and pore volumes of nanocrystals prepared with 25% Cu doping were found to be lower than those measured with weaker doping percentage in Cu. Finally, pore size distribution (calculated by the Horvath-Kawazoe method) are centered around 1.2 nm and perfectly agree with that from the ZIF-8 structural model.

Table 1 Comparison of BET, pore volume, and pore size for ZIF-8 and Cu-doped ZIF-8 crystals

Material	BET^{a,b} (m^2g^{-1})	Pore volume^b (cm^3g^{-1})	Pore size^b (nm)
ZIF-8	1700 ± 30	0.662	1.2922
$Cu_{1\%}$/ZIF-8	1541 ± 40	0.518	1.2214
$Cu_{5\%}$/ZIF-8	1736 ± 59	0.601	1.2179
$Cu_{10\%}$/ZIF-8	1639 ± 56	0.571	1.2169
$Cu_{25\%}$/ZIF-8	1205 ± 47	0.440	1.2190

^{a} BET surface area. ^{b} Values are the average of two experiments.
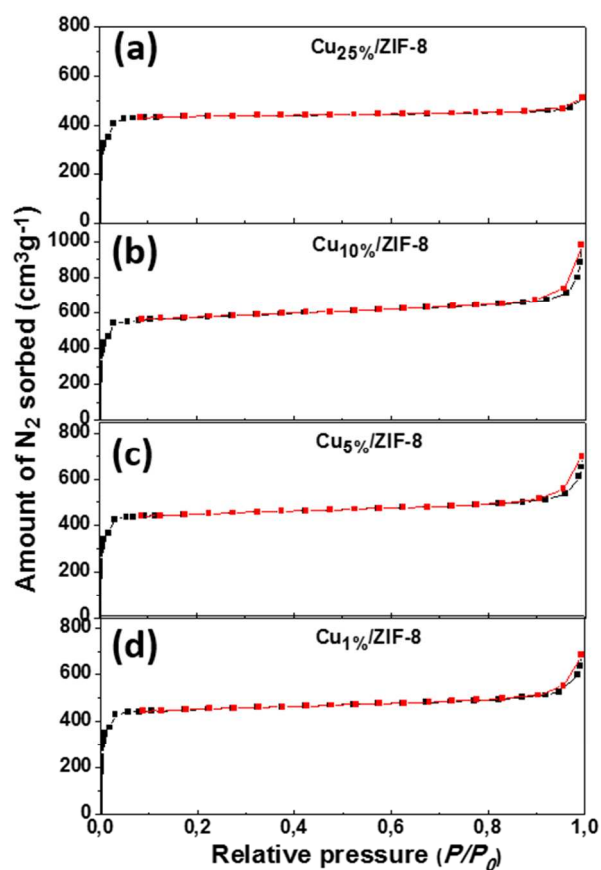
Fig. 7 N_2 adsorption/desorption curves at 77K for Cu/ZIF materials doped with (a) 25% Cu, (b) 10% Cu, (c) 5% Cu, and (d) 1% Cu, giving surface areas of 1205, 1639, 1736, and 1541 m^2 g^{-1}, respectively. Black and red data correspond to the adsorption and desorption branches, respectively.

The thermogravimetric analyses coupled to mass spectrometry (TGA/MS) of ZIF-8 and Cu/ZIF-8 samples only differ slightly (Fig. S2). From 20 to 200°C, the TGA curves exhibited only a very weak weight loss of less than 0.5%, corresponding to the removal of guest molecules (methanol or Hmim and/or CO_2 from

the cavities as indicated by MS analyses). A long plateau was then observed after the formation of the guest-free $Cu/Zn(mim)_2$ crystals until 350°C, indicating good thermal stability of the three-dimensional network for all samples, which is comparable to the literature.[14,19] All curves exhibit one step which can be assigned to the decomposition of the mim^- linker above 350°C (onset of the exothermic decomposition). The sharp weight loss of ca. 63-64% observed upon increasing the temperature from 400 to 500°C is in good agreement with the theoretical weight loss of 64%. The residue is wurtzite Cu-doped ZnO as proven by XRD measurements. It is also worth to mention that Cu/ZIF-8 crystals from this work exhibit higher thermal stability than Cu-based MOFs like Cu(BDC) used for catalytic applications, which already decompose at 200°C.[27]

Finally, the chemical stability of Cu/ZIF-8 crystals was evaluated by dispersing the samples in boiling water, 1M NaOH, toluene or methanol, conditions that reflect extreme operational parameters of typical industrial chemical process. Powder XRD patterns recorded for each sample after one week heating indicate that the topology of the ZIF-8 framework is preserved in 1M NaOH, toluene or methanol. Only the sample heated in water at neutral pH gradually decomposed into ZnO (see Fig. S3).

Cu/ZIF-8 particles as catalysts for Friedländer and Combes condensations

The catalytic activity of Cu/ZIF-8 crystals was first evaluated in the copper-catalyzed synthesis of quinoline derivatives, heterocycles of high interest due to their broad range of pharmaceutical and biological activities.[61-64] We carried out the condensation of 2-aminobenzophenone with acetylacetone or ethyl acetoacetate in the presence of Cu/ZIF-8 crystals (Scheme 2).
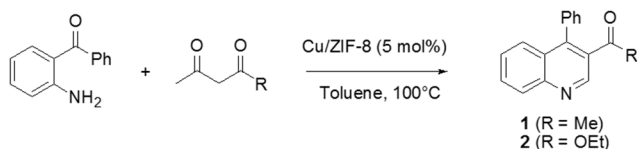
Scheme 2 Cu/ZIF-8 catalyzed Friedländer reactions between 2-aminobenzophenone and active methylene compounds.

The reactions were conducted using a 2-aminobenzophenone/active methylene compound molar ratio of 1/1.5 and in toluene at 100°C. Poor conversion of 2-aminobenzophenone (less than 10%) was observed with the $Cu_{1\%}$/ZIF-8 material but the reaction proceeded efficiently in 8 h with $Cu_{5\%}$/ZIF-8 crystals yielding compounds **1** and **2** in quantitative yields. In addition, although the final yields of **1** and **2** when operating with catalysts containing a higher copper percentage (10 or 25%) were almost the same, the reaction times were reduced to ca. 5 h. It is also worth to mention that products **1** and **2** of the Friedländer condensation were not obtained in control experiments carried out either without catalyst or with ZIF-8 crystals. Cu^{2+} ions, acting as Lewis acids in the Friedländer reaction, are randomly located in the Cu/ZIF-8 crystals. Poor results obtained with the $Cu_{1\%}$/ZIF-8 material seem to indicate that the reaction proceeds on the external surface of the catalyst

and that Cu^{2+} ions located in the pores are probably not accessible to reactants. With the increase of Cu^{2+} doping, more of these ions should be present at the surface of the Cu/ZIF-8 catalyst and its activity increased. To confirm the key role of Cu^{2+} species in the Friedländer reaction, we carried out the condensation of 2-aminobenzophenone with ethyl acetoacetate in the presence of 100 equivalents of pyridine relative to the Cu/ZIF-8 catalyst. In the presence of the pyridine catalyst poison, the quinoline **2** was not detected, thus indicating that pyridine strongly bounds and completely blocks catalytically active Cu^{2+} sites. Finally, to demonstrate that the Cu/ZIF-8 is a real heterogeneous catalyst and that catalytically active Cu^{2+} ions are not leaked in the medium during the course of the reaction, a centrifugation was carried out after 15 min of reaction and the catalyst separated. No further conversion of starting materials was observed upon further heating the supernatant at 100°C, thus confirming that the condensation is mediated by a heterogeneous catalyst.

We also investigated different catalyst loadings in the course of the reaction leading to quinoline **2** and found that 8 mol% $Cu_{5\%}$/ZIF-8 afforded the best results. Decreasing the amount of $Cu_{5\%}$/ZIF-8 led to lower yields of **1** and **2**, therefore the optimum catalyst amount was kept at 8 mol%.

We next studied the Combes condensation using Cu/ZIF-8 as catalyst of aniline with acetylacetone leading to 2,4-dimethylquinoline **3** (Scheme 3). Since both starting materials are liquid, the reaction was carried out under solvent-free conditions using an excess of acetylacetone (5 equiv.). Quinoline **3** was isolated in 96% yield after column chromatography using the $Cu_{5\%}$/ZIF-8 catalyst for 5 h at 100°C. As previously observed during the Friedländer condensations, product **3** was not detected in the absence of catalyst or with ZIF-8.
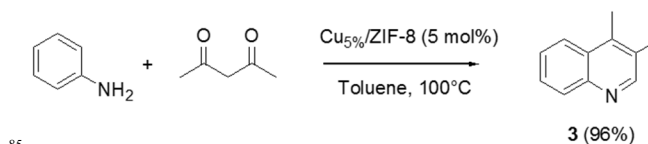
Scheme 3 Cu/ZIF-8-catalyzed Combes reaction between aniline and acetylacetone.

Finally, we checked the reusability of Cu/ZIF-8 as heterogeneous catalyst in Friedländer and Combes reactions yielding products **2** and **3**, respectively. After the reaction, the catalyst was recovered by centrifugation, washed with ethanol, dried at 70°C and used for another consecutive run without further treatment. In both cases, the catalyst exhibited no decrease in activity after five runs. As shown in Fig. 8, the shape and the crystallinity of the particles after the five cycles remained unchanged, thus showing its stability and recyclability. A strong decrease in catalytic activity was only observed after the 10th run (44%). After five recyclings in the Combes reaction, the textural properties of the $Cu_{5\%}$/ZIF-8 material were evaluated by N_2 adsorption-desorption isotherm at 77K. The curve obtained for the catalyst remained a typical type-I isotherm (see Fig. S4), indicating that the particles maintained their micropores. The value of S_{BET} decreased from 1639 to 1030 $m^2.g^{-1}$ after the 5th run, probably due to the irreversible adsorption of reagents and/or by-products at the surface of the catalyst.

Cu/ZIF-8 crystals in 1,3-dipolar cycloadditions

Huisgen's dipolar cycloaddition (click reaction) between organic azides and alkynes is the most important synthetic route to 1,2,3-triazoles.[65] The discovery that copper(+1) efficiently catalyses this cycloaddition providing triazoles under mild conditions and the 1,4-isomer with high regioselectivity was a welcome advance.[66,67] In recent years, click reactions have found many applications in chemistry, biology and materials science.[68-70] Cu(+2) in the absence of reducing agent like ascorbate can also catalyse the
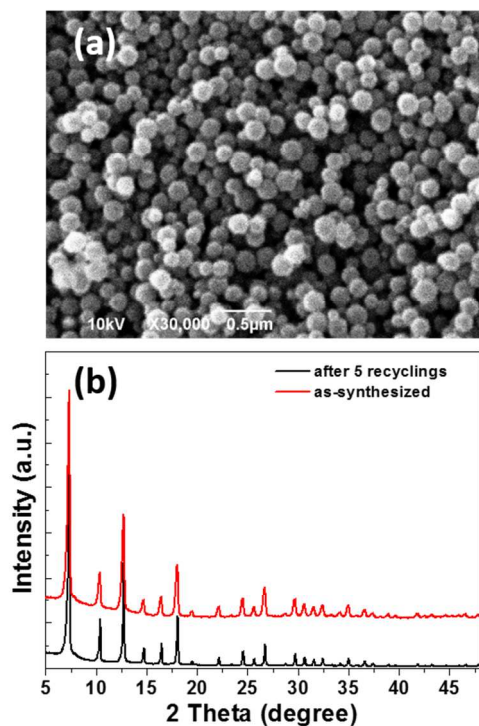

Fig. 8. (a) SEM image of ZIF-8 crystals after five reuses in the Combes condensation and (b) XRD patterns of as-synthesized ZIF-8 (red) and ZIF-8 crystals after five reuses (black) in the Combes condensation.

cycloaddition of azides and alkynes but this reaction generally suffers from drawbacks like high catalyst loading and low yield compared to Cu(+1)-catalyzed reactions.[71-75] In these screens, a mixture of benzylazide and phenylacetylene (1:1.2 equiv, respectively) was heated in toluene at 100°C for 3 h in the presence of 5 mol% of the Cu/ZIF catalyst. The resulting mixture was next analyzed by ^{1}H NMR. As shown in Table 2, we were pleased to find out that Cu/ZIF-8 crystals catalyse the formation of 1,2,3-triazoles with catalytic activity and regioselectivity being dependent on the Cu dopant percentage. With the $Cu_{25\%}$/ZIF-8 catalyst, the consumption of benzylazide was complete and the 1,4-isomer was obtained with a high regioselectivity (92/8). Under similar experimental conditions, undoped ZIF-8 crystals were completely ineffective in catalysing the cycloaddition and no trace of triazole was detected even after 24 h heating in toluene at 100°C.

We next evaluated the scope of this new Cu/ZIF-8 catalyzed process. All reactions were performed with 5 mol% of

$Cu_{25\%}$/ZIF-8 in toluene at 100°C. As can be seen in Table 3, various combinations of organic azides and alkynes were efficiently converted into the corresponding disubstituted triazoles without any additive. Not only benzylic but also aliphatic azides gave excellent yields. Aliphatic alkynes worked also well as reaction partners of organic azides. The regioselectivity was good, varying from 78/22 to 95/5. After reaction, the $Cu_{25\%}$/ZIF-8 particles were separated through centrifugation and used in click reactions between phenylacetylene and octylazide without loss of catalytic activity during five cycles.
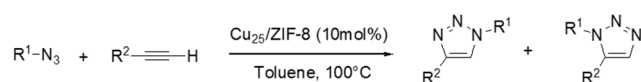
Table 2 Influence of the Cu-doping on the regioselectivity of cycloadditions catalysed by Cu/ZIF-8 crystals.
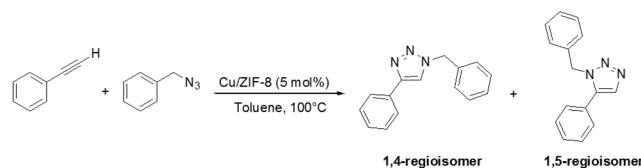
Catalyst	1,4-regioisomer[a]	1,5-regioisomer[a]	Yield[b] (%)
$Cu_{1\%}$/ZIF-8	45	55	79
$Cu_{5\%}$/ZIF-8	50	50	98
$Cu_{10\%}$/ZIF-8	62	38	99
$Cu_{25\%}$/ZIF-8	92	8	99

[a] Percentages determined by ^{1}H NMR. [b] Isolated yields after column chromatography.

Table 3 Synthesis of 1,2,3-triazoles using Cu/ZIF-8 particles.

R^1	R^2	1,4/1,5[a]	Yield[b] (%)
Bn	Ph	92/8	99
Octyl	Ph	79/21	90
Octyl	$SiMe_3$	95/5	84
$H_3CO-C(O)-(CH_2)_3-$	Ph	78/22	97

[a] Percentages determined by ^{1}H NMR. [b] Isolated yields after column chromatography.

Conclusions

In summary, we have demonstrated that ZIF-8 crystals could be easily doped with Cu^{2+} ions (between 1 and 25%) without alteration of ZIF-8 thermostability (up to 350°C in air) and crystallinity. An increase of ZIF-8 particles from ca. 120 to 170 nm was observed when increasing the dopant percentage from 1 to 25%. Until 10% doping in copper, the permanent porosities of Cu/ZIF-8 particles were not altered but decreased slightly from

ca. 1600 to 1200 m^2.g^{-1} when 25% Cu^{2+} relative to Zn^{2+} was used. Importantly, Cu/ZIF-8 particles were proven to be efficient and reusable catalysts for the [3+2] cycloaddition of organic azides with alkynes and for Friedländer and Combes condensations. The Cu$_{5\%}$/ZIF-8 crystals showed high catalytic activity in the synthesis of quinolines using 2-aminobenzophenone as starting material. 1,4-Disubstituted triazoles were obtained with excellent yields and good regioselectivity using the Cu$_{25\%}$/ZIF-8 material. These results combined with the high stability and the ease of regeneration of ZIF-8 particles may serve as a starting point to develop new nanomaterials based on metal organic frameworks with high adsorbent properties and enhanced catalytic properties.

Acknowledgements

Notes and references

^{a} *Laboratoire Réaction et Génie des Procédés (LRGP), UMR CNRS 7274, Université de Lorraine, 1 rue Grandville 54001 Nancy, France. Tel: +33 3 83 17 50 53; E-mail: raphael.schneider@univ-lorraine.fr*
^{b} *Clermont Université, Université Blaise Pascal, Institut de Chimie de Clermont-Ferrand, 24 Avenue des Landais, BP 80026, 63174, Aubière, France.*
^{c} *Institut de Science des Matériaux de Mulhouse (IS2M), UMR 7361, CNRS, 15 rue Jean Starcky, 68093 Mulhouse, France*
^{d} *Institut Jean Lamour (IJL), Université de Lorraine, CNRS, UMR 7198, CNRS, BP 70239, 54506 Vandoeuvre-lès-Nancy Cedex, France*

† Electronic Supplementary Information (ESI) available: Size distributions of Cu/ZIF-8 crystals and XRD patterns of crystals after chemical treatment. See DOI: 10.1039/b000000x/

1   J. S. Sco, D. Whang, H. Lee, S. I. Jun, J. Oh, Y. J. Leon and K. Kim, *Nature*, 2000, **404**, 982-986.
2   H. Hayshi, A. P. Cote, H. Furukawa, M. O. O'Keeffe and O. M. Yaghi, *Nat. Mater.*, 2007, **6**, 501-506.
3   P. K. Thallapally, J. Tian, M. R. Kishan, C. A. Fernandez, S.J. Dalgarho, P.B. Mc Grail, J. E. Warren and J. L. Atwood, *J. Am. Chem. Soc.*, 2008, **130**, 16842-16843.
4   D. Britt, D. Tranchemontagne and O. M. Yaghi, *Proc. Natl. Acad. Sci. U.S.A.*, 2008, **105**, 11623-11627.
5   D. Britt, H. Furukawa, B. Wang, G. Glover and O. M. Yaghi, *Proc. Natl. Acad. Sci. U.S.A.*, 2009, **106**, 20637-20640.
6   J. -R. Li, R. J. Kuppler and H. -C. Zhou, *Chem. Soc. Rev.*, 2009, **38**, 1477-1504.
7   Z. H. Xiang, D. P. Cao, J. H. Lan, W. C. Wang and D. P. Broom, *Energy Environ. Sci.*, 2010, **3**, 1469-1487.
8   S. Benmansour, C. Atmani, S. Setifi, S. Triki, M. Marchivie and C. Gomez-Garcia, *J. Coord. Chem. Rev.*, 2010, **254**, 1468-1478.
9   R. Morris and P. Wheatley, *Angew. Chem. Int. Ed.*, 2008, **47**, 4966-4981.
10 O. K. Farha, A. O. Yazaydin, I. Eryazici, C. D. Malliakas, B. G. Hauser, M. G. Kanatzidis, S. T. Nguyen, R. Q. Snurr and J. T. Hupp, *Nat. Chem.*, 2010, **2**, 944-948.
11 B. Chen, C. Liang, J. Yang, D. S. Contreras, Y. L. Clancy, E. B. Lobkovsky, O. M. Yaghi and S. A. Dai, *Angew. Chem. Int. Ed.*, 2006, **45**, 1390-1393.
12 J. Lee, O. K. Farha, J. Roberts, K. A. Scheidt, S. T. Nguyen and J. T. Hupp, *Chem. Soc. Rev.*, 2009, **38**, 1450-1459.
13 N. Liédana, A. Galve, C. Rubio and J. Coronas, *ACS Appl. Mater. Interfaces*, 2012, **4**, 5016-5021.
14 K. S. Park, Z. Ni, A. P. Côté, J. Y. Choi, R. D. Huang, F. J. Uribe-Romo, H. K. Chae, M. O'Keeffe and O. M. Yaghi, *Proc. Natl. Acad. Sci. U.S.A.*, 2006, **103**, 10186-10191.
15 X. C. Huang, Y. Y. Lin, J. P. Zhang and X. M. Chen, *Angew. Chem. Int. Ed.*, 2006, **45**, 1557-1559.
16 B. Wang, A. P. Côté, H. Furukawa, M. O'Keeffe and O. M. Yaghi, *Nature*, 2008, **453**, 207-211.
17 R. Banerjee, A. Phan, B. Wang, C. Knobler, H. Furukawa, M. O'Keeffe and O. M. Yaghi, *Science*, 2008, **319**, 939-943.
18 H. Wu, W. Zhou and T. Yildirim, *J. Am. Chem. Soc.*, 2007, **129**, 5314-5315.
19 A. Schejn, L. Balan, V. Falk, L. Aranda, G. Medjahdi and R. Schneider, *CrystEngComm*, 2014, **16**, 4493-4500.
20 H. -L. Jiang, B. Liu, T. Akita, M. Haruta, H. Sakurai and Q. Xu, *J. Am. Chem. Soc.*, 2009, **131**, 11302-11303.
21 D. Esken, H. Noei, Y. Wang, C. Wiktor, S. Turner, G. Van Tendeloo and R. A. Fischer, *J. Mater. Chem.*, 2011, **21**, 5907-5915.
22 D. Esken, S. Turner, C. Wiktor, S. B. Kalidindi, G. Van Tendeloo and R. A. Fischer, *J. Am. Chem. Soc.*, 2011, **133**, 16370-16373.
23 G. Lu, S. Li, O. K. Farha, B. G. Hauser, X. Qi, Y. Wang, X. Wang, S. Han, X. Liu, J. S. DuChene, H. Zhang, Q. Zhang, X. Chen, J. Ma, S. C. J. Loo, W. D. Wei, Y. Yang, J. T. Hupp and F. Huo, *Nat. Chem.*, 2012, **4**, 310-316.
24 Z. Li and H. C. Zeng, *Chem. Mater.*, 2013, **25**, 1761-1768.
25 L. Chen, Y. Peng, H. Wang, Z. Gu and C. Duan, *Chem. Commun.*, 2014, **50**, 8651-8654.
26 F. Wang, Z. -S. Liu, H. Yang, Y. -X. Tan and J. Zhang, *Angew. Chem. Int. Ed.*, 2011, **50**, 450-453.
27 I. Luz, F. X. Llabrés i Xamena and A. Corma, *J. Catal.*, 2010, **276**, 134-140.
28 I. Luz, F. X. Llabrés i Xamena and A. Corma, *J. Catal.*, 2012, **285**, 285-291.
29 Y. Wu, L. -G. Qiu, W. Wang, Z. -Q. Li, T. Xu, Z. -Y. Wu and X. Jiang, *Transition Met. Chem.*, 2009, **34**, 263-268.
30 A. Dhakshinamoorthy, M. Alvaro and H. Garcia, *J. Catal.*, 2009, **267**, 1-4.
31 N. Masciocchi, S. Bruni, E. Cariati, F. Cariati, S. Galli and A. Sironi, *Inorg. Chem.*, 2001, **40**, 5897-5905.
32 J. Fan, L. Gan, H. Kawaguchi, W. -Y. Sun, K. -B. Yu and W. -X. Tang, *Chem. Eur. J.*, 2003, **9**, 3965-3973.
33 J. Fan, W. -Y. Sun, T. -a. Okamura, W. -X. Tang and N. Ueyama, *Inorg. Chem.*, 2003, **42**, 3168-3175.
34 W. Zhao, J. Fan, T. -a. Okamura, W. -Y. Sun and N. Ueyama, *New J. Chem.*, 2004, **28**, 1142-1150.
35 L. -F. Ma, Q. -L. Meng, L. -Y. Wang and F. -P. Liang, *Inorg. Chim. Acta*, 2010, **363**, 4127-4133.
36 H. -j. Pang, H. -y. Ma, J. Peng, C. -j. Zhang, P. -p. Zhang and Z. -m. Su, *CrystEngComm*, 2011, **13**, 7079-7085.
37 Y. Zhu, W. -y. Wang, M. -w. Guo, G. Li and H. -j. Lu, *Inorg. Chem. Commun.*, 2011, **14**, 1432-1435.
38 J. Xu, X. -Q. Yao, L. -F. Huang, Y. Z. Li and H. -G. Zheng, *CrystEngComm*, 2011, **13**, 857-865.
39 H. Fu, Y. Li, Y. Lu, W. Chen, Q. Wu, J. Meng, X. Wang, Z. Zhang and E. Wang, *Cryst. Growth Des.*, 2011, **11**, 458-465.
40 S. -S. Chen, M. Chen, S. Takamizawa, M. -S. Chen, Z. Su and W. -Y. Sun, *Chem. Commun.*, 2011, **47**, 752-754.
41 A. Béziau, S. A. Baudron, D. Pogozhev, A. Fluck and M. W. Hosseini, *Chem. Commun.*, 2012, **48**, 10313-10315.
42 L. Wen, J. Zhao, K. Lv, Y. Wu, K. Deng, X. Leng and D. Li, *Cryst. Growth Des.*, 2012, **12**, 1603-1612.
43 H. -Y. Lin, B. Mu, X. -L. Wang and A. -X. Tian, *J. Organomet. Chem.*, 2012, **702**, 36-44.
44 D. -D. Zhou, C. -T. He, P. -Q. Liao, W. Xue, W. -X. Zhang, H. -L. Zhou, J. -P. Zhang, and X. -M. Chen, *Chem. Commun.*, 2013, **49**, 11728-11730.

45   A. Vlad, M. -F. Zaltariov, S. Shova, G. Novitchi, C. -D. Dragoa, C. Train and M. Cazacu, *CrystEngComm*, 2013, **15**, 5368-5375.

46   Z. -H. Li, L. -P. Xu, L. Wang, S. -T. Zhang and B. -T. Zhao, *Inorg. Chem. Commun.*, 2013, **27**, 119-121.

47   S. K. Chawla, M. Arora, K. Nättinen, K. Rissanen and J. V. Yakhmi, *Polyhedron*, 2004, **23**, 3007-3019.

48   J. -F. Song, Y. Chen, Z. -G. Li, R. -S. Zhou, X. -Y. Xu and J. -Q. Xu, *J. Mol. Struct.*, 2007, **842**, 125-131.

49   H. Yang, X. -W. He, F. Wang, Y. Kang and J. Zhang, *J. Mater. Chem.*, 2012, **22**, 21849-21851.

50   R. Li, X. Ren, H. Ma, X. Feng, Z. Lin, X. Li, C. Hu and B. Wang, *J. Mater. Chem. A*, 2014, **2**, 5724-5727.

51   R. Li, X. Ren, X. Feng, X. Li, C. Hu and B. Wang, *Chem. Commun.*, 2014, **50**, 6894-6897.

52   D. M. Schubert, D. T. Natan and C. B. Knobler, *Inorg. Chim. Acta*, 2009, **362**, 4832-4836

53   E. J. O'Neil, K. M. DiVittorio and B. D. Smith, *Org. Lett.*, 2007, **9**, 199-202.

54   D. L. Versace, J. Lalevée, J. -P. Fouassier, Y. Guillaneuf, D. Bertin and D. Gigmes, *Macromol. Rapid Comm.*, 2010, **31**, 1383–1388.

55   S. R. Vanna, J. B. Jasinski and M. A. Carreon, *J. Am. Chem. Soc.*, 2010, **132**, 18030-18033.

56   J. Cravillon, S. Münzer, S. J. Lohmeier, A. Feldhoff, K. Huber
57   and M. Wiebcke, *Chem. Mater.*, 2009, **21**, 1410-1412.

58   L. Zhang and Y. H. Hu, *J. Phys. Chem. C*, 2011, **115**, 7967-7971.

59   D. Li, S. Li, D. Yang, J. Yu, J. Huang, Y. Li and W. Tang, *Inorg. Chem.*, 2003, **42**, 6071-6080.

60   Y. -C. Fang, H. -C. Lin, I. -J. Hsu, T. -S. Lin and C. -Y. Mou, *J. Phys. Chem. C*, 2011, **115**, 20639-20652.

61   K. S. W. Sing, D. H. Everett, R. A. W. Haul, L. Moscou, R. A. Pierotti, J. Rouquérol and T. Siemieniewska, *Pure Appl. Chem.*, 1985, **57**, 603-619.

62   M. Barbero, S. Bazzi, S. Cadamuro and S. Dughera, *Tetrahedron Lett.*, 2010, **51**, 2342-2344.

63   H. V. Mierde, P. V. D. Voort and F. Verpoort, *Tetrahedron Lett.*, 2008, **49**, 6893-6895.

64   F. O'Donnell, T. J. P. Smyth, V. N. Rama-Chandran and W. F. Smyth, *J. Antimicrob. Agents*, 2010, **35**, 30-38.

65   A. Busatti, D. E. Crawford, M. J. Earle, M. A. Gilea, B. F. Gilmore, S. P. Gorman, G. Laverty, A. F. Lowry, M. McLaughlin and K. R. Seddon, *Green Chem.*, 2010, **12**, 420-425.

66   R. Huisgen, In 1,3-Dipolar Cycloaddition Chemistry ; Padwa, A.; Ed.; Wiley: New York, 1984.

67   V. V. Rostovtsev, L. G. Green, V. V. Fokin and K. B. Sharpless, *Angew. Chem. Int. Ed.*, 2002, **41**, 2596-2599.

68   C. W. Tornoe, C. Christensen and M. Meldal, *J. Org. Chem.*, 2002, **67**, 3057-3064.

69   G. C. Tron, T. Pirali, R. A. Billington, P. L. Canonico, G. Sorba and A. A. Genazzani, *Med. Res. Rev.*, 2008, **28**, 278-208.

70   J. E. Moses and A. D. Moorhouse, *Chem. Soc. Rev.*, 2007, **36**, 1249-1262.

71   P. Thirumurugan, D. Matosiuk and K. Jozuwiak, *Chem. Rev.*, 2013, **113**, 4905-4979.

72   M. -C. Ye, J. Zhou, Z. -Z. Huang and Y. Tang, *Chem. Commun*, 2003, 2554-2555.

73   J. A. Gladysz, *Chem. Rev.*, 2002, **102**, 3215-3216.

74   A. T. Bell, *Science*, 2003, **299**, 1688-1691.

75   R. Schlögl and S. B. A. Hamid, *Angew. Chem. Int. Ed.*, 2004, **43**, 1628-1637.

76   J. Y. Kim, J. C. Park, H. Kang, H. Song and K. H. Park, *Chem. Commun.* 2010, **46**, 439-441.